

TECHNICAL NOTE: AN-922

(IFPAC-2001, Paper I-020, January 21-24, 2001)

COMPARISON OF NEAR-IR AND RAMAN ANALYSIS FOR POTENTIAL PROCESS APPLICATIONS

**W. M. Doyle
Axiom Analytical, Inc.**

Abstract

Near-infrared and Raman spectroscopy are complimentary techniques with considerable potential for on-line process analysis. Near-IR, in fact, has already gained wide acceptance for the analysis of commodity chemicals and other products that can justify the often considerable cost of near-IR calibrations. Raman spectroscopy offers the potential of much simpler calibrations. However, its application to process analysis has been held back to some extent by the less mature nature of the instrumentation. This situation is now starting to change as both the instruments and sampling equipment become more hardened. As a result, Raman is becoming a viable alternative to Near-IR for many dedicated applications. The present paper evaluates the potential of both near-IR and Raman for potential process applications involving a variety of sample types. Experimental data is provided which compares the utility of each technique for samples ranging from granular solids to heterogeneous mixtures.

1. INTRODUCTION:

Both near infrared and Raman spectroscopy are finding steadily increasing application to a wide range of industrial applications. The general characteristics of these two analytical techniques are fairly well known. As a result, the choice of which technique to apply can sometimes be made on a routine basis once the general nature of the sample system is known. However, in many other cases, the choice is not at all obvious and a more thorough analysis may be needed. The object of this paper is to address some of these cases and to provide guidelines that may help simplify the process.

Near-infrared and Raman are two of the three common forms of molecular spectroscopy, the third being mid-infrared. The characteristics of all three are summarized in a simplified form in Table I. Simplifying further, we can state that the major attractiveness of NIR resides in the availability of fiber-optics for near-IR signal transmission. Mid-IR, on the other hand encompasses the fundamental vibrational bands of all organic molecules. As a result, mid-IR calibrations tend to be simple and robust. The problem with Near-IR is not, as is often stated, that the overtone and combination tone bands are broad. It is rather a result of the overlap of the various orders of the overtones. Only vibrations involving very light atoms (eg. CH and OH) have first overtones in the near-IR region. And these usually swamp the much weaker second, third, and fourth overtones of the fingerprint spectra falling in the same spectral region. Thus near-IR calibrations tend to be quite tedious and often require continuous maintenance.

TABLE I: MOLECULAR SPECTROSCOPY CHARACTERISTICS

	Mid-IR	Near-IR	Raman
Bands	Fundamentals	Overtones of CH	Fundamentals
Calibrations	Simple	Tedious	Simple
Sampling Method	ATR	Transmission	Backscatter
Optics	Sensitive	Resilient	Resilient
Fiber-optics	Not practical	OK	OK
Fluorescence	OK	OK	Can be a problem
Referencing	OK	OK	Can be a problem
Hardware Maturity	Moderate	Good	Early Stage

Raman spectroscopy, while at a somewhat earlier stage of hardware maturity, combines the convenience of practical fiber-optic signal transmission with the specificity of fundamental bands. It thus shares the attractive features of both mid-IR and near-IR. It does, however, have some weaknesses. These will be discussed in some detail below.

Table II summarizes the applicability of near-IR and Raman spectroscopy to samples in various physical forms. Here we have made a distinction between near-IR transmission and diffuse reflectance. Near-IR transmission has two very desirable characteristics. First, adherence to Beer's law makes transmission data relatively manageable. Second it is a well established and generally very reliable method with mature hardware and relatively low cost of ownership. As a result, Near-IR transmission will generally be the method of choice for the analysis of clear fluids. I thus will devote the bulk of this paper to sample system to which near-IR transmission does not apply. These include granular and bulk solids and heterogeneous mixtures. The issues in these cases include data linearization and normalization, uncertainties due to sample form, the effects of a fluid matrix, the dependence of the measurement on viewed area, and the information content of the data.

TABLE II: APPLICABILITY OF FIBER-OPTIC COUPLED ANALYTICAL TECHNIQUES

Sample Type	NIR Transmission	Diffuse Reflectance	Raman
Clear Fluids	Yes	No	Yes
Scattering Fluids	Some Cases	Some Cases	Yes
Granular Solids	No	Yes	Yes
Bulk Solids, Scattering	No	Yes	Yes
Bulk Solids, Clear	Some Cases	No	Yes

THE NATURE OF THE SPECTRA:

The adherence of transmission spectral data to Beer's law has two important consequences. First the data can be converted to a form which is linear in concentration by simply taking the negative log. Once linearized, it can be analyzed by means of the various multivariate (chemometric) data reduction programs available. Second, the log function converts multiplicative errors into additive errors, which can easily be ignored. This is important since measurement artifacts – such as those resulting from source fluctuations or degradation of instrument or sampling optics – will typically be multiplicative.

Neither Raman nor diffuse reflectance spectra follow Beer's law. In the case of Raman, the raw spectra of homogeneous samples are linear in concentration. This, at first, may appear to be advantageous. However, it does present a problem in that multiplicative errors can mimic concentration changes. The only safe way to mitigate this problem is to use the internal characteristics of the data itself to normalize the measurements. In the case of a chemical reaction in which some molecular bonds are not effected by the reaction, a varying band can be normalized by dividing it by a constant band. Below, I will describe another approach to normalization, which is applicable to mixtures of non-reacting substances.

Although diffuse reflectance spectra do not follow Beer's law, they can often be linearized by using the Kubelka-Munk function:

$$F(R^\infty) = (1-R)^2/2R,$$

where "R" is the measured reflectance. The utility of the Kubelka-Munk function resides in the fact that it is proportional to concentration in certain idealized cases, most notably situations in which the scattering characteristics of all of the samples are the same (Ref. 1). In such cases, the linearized data can then be subjected to chemometric analysis. However, caution should be exercised in applying the Kubelka-Munk function since multiplicative errors in measured reflectance do not translate into additive errors and hence can not be ignored. This is analogous to the multiplicative error problem in Raman spectroscopy. And, as in the Raman case, it necessitates appropriate normalization.

So far, I have noted two similarities between near-IR and Raman analysis. In both cases, the data are generally amenable to chemometric analysis as long as the materials being analyzed are homogeneous. And both require some form of normalization to remove uncertainties caused by multiplicative errors. As we will see below, the similarities go even further. In both cases, the data can be very highly non-linear in concentration if the samples are inhomogeneous – i.e. if they involve mixtures of substances having different scattering characteristics. As is illustrated in reference 1, diffuse reflectance spectra depend on both the absorption and scattering characteristics of each substance present. If the scattering characteristics of the various components are substantially different, the dependence on concentration will be highly nonlinear, albeit in a predictable way. As I will illustrate below, similar considerations apply to Raman spectra; although the functionality of the scattering dependence will be substantially different.

There are a number of obvious ways in which near-IR and Raman spectra differ. These can have bearing on the relative utility of the two techniques for particular measurements. The more important of these are listed below:

Near-IR Diffuse Reflectance Limitations:

The functionalities of diffuse reflectance spectra on concentration are only easily predictable when the various assumptions underlying the Kubelka-Munk theory apply. In particular, diffuse reflectance spectra can be distorted by such factors as:

- specular reflectance
- limited sample illumination and viewed area
- limited thickness
- particle size
- refractive index variations
- inhomogeneity

Raman Limitations:

Raman spectra may be obscured or degraded if any of the follow are present:

- sample fluorescence
- pigmentation at either the laser or Raman shift frequencies
- background illumination
- high temperatures
- unpredictable or frequency dependent diffuse scattering

NIR AND RAMAN ANALYSIS OF HOMOGENEOUS SAMPLES:

The choice of analytical technique is simplified if the analyte is either a clear liquid or solid or a uniform powder. In these cases, there are still a number of factors that need to be considered. But these are generally well understood and can be clearly weighed in determining the approach most likely to succeed.

Raman will typically be preferred if the samples are transparent bulk solids. Near-IR transmission can also be applied in some cases, but it requires that the surfaces be flat and parallel and that the sample be limited in thickness and of uniformly good optical quality. The use of Raman may be dictated if the analyte lacks a near IR spectrum (e.g. many inorganics) or if the near-IR spectrum has insufficient specificity for the required analysis. This will often be the case if the physical or chemical properties of interest have very subtle spectral effects. Finally, Raman may be preferred if the process cannot justify the cost of the Near-IR calibration required. This will often be the case if a given process system is used for a number of different short production runs or in process development applications where it is necessary to screen a large number of reactions or materials.

Near-IR transmission will often be preferred for clear liquids due to the maturity and reliability of the hardware and the fact that adherence to Beer's law greatly aids data treatment. Of course, Raman may still be preferred for rapid screening and other applications requiring simple calibrations, as noted above.

Near-IR diffuse reflectance will generally be preferred for scattering solids for which Raman is problematic due to such factors as fluorescence, pigmentation, or background

radiation. It may also be preferred in cases where a very large sampling area is needed due to sample inhomogeneity. In many other applications involving particulate matter, it may be necessary to experimentally evaluate both approaches before making a decision. This is particularly true of inhomogeneous mixtures, i.e. mixtures of substances having different scattering characteristics. Several examples are examined below.

SPECIFIC COMPARISONS OF NEAR-IR AND RAMAN ANALYSIS:

Effects of physical form and limited sampling area:

Many applications require monitoring of particulate material – such as polymer pellets – which may be traveling through a pipe or on a conveyor belt. Analyses of this type have been successfully carried out over the years by using near-IR diffuse reflectance. In most cases it has been necessary to use an illumination area which is large compared to the particle size. While the exact requirement depends on required accuracy of the measurement, a rule of thumb that is often applied is that the diameter of the illuminated and viewed area should be at least a hundred times the typical particle diameter. This approach works best when the analyzer can be located adjacent to the process and coupled to it either by one or more large diameter fiber bundle or by discrete optical elements. However, for most process measurements, it is highly desirable to locate the instrument in a controlled environment remote from the process. In such cases there will be a critical trade-off between illuminated area and received signal level (Ref. 2).

To illustrate the trade-off between sampling area and measurement repeatability, we acquired multiple spectra of polyethylene granules with various particle sizes and illuminated areas. To do this we used a prototype diffuse reflectance probe coupled to the near-IR spectrometer by means of a 2.5 mm diameter bifurcated fiber-optic bundle. The particular probe design used allows the spot diameter to be varied between 2.5 mm and 32 mm.

Figure 1 is a set of overlaid spectra corresponding to five different areas of 0.5 to 1 mm diameter granules viewed with 32 mm diameter illumination. Figure 2 represents the same sort of measurements except with 3 to 4 mm diameter granules and a 10 mm diameter illuminated area. The differences both in the gross characteristics of the spectra and in their repeatability are dramatic. First, the absorption bands seen in Figure 2 are much stronger than those in Figure 1. This is due to the reduced scattering and hence greater penetration depth that occurs with the larger particles. Second the signal level in spectral regions of low absorption is substantially reduced due to the fact that some of the radiation is scattered out of the field of view of the receiving optics. The magnitude of this effect varies significantly with different viewing areas. Third, in the region very strong absorption, we see a baseline off-set due to specular reflectance. This also varies with view area.

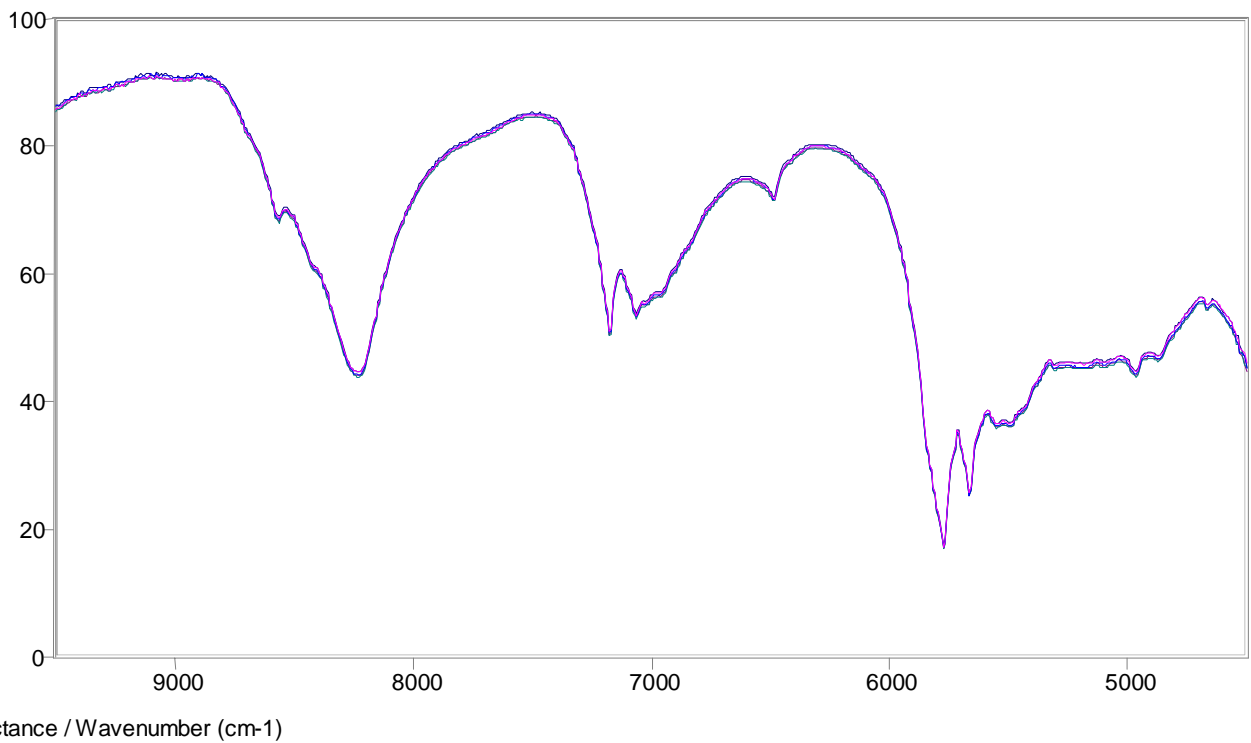


Figure 1: Diffuse reflectance spectra of five different areas of granular polyethylene obtained with a 32 mm spot size.

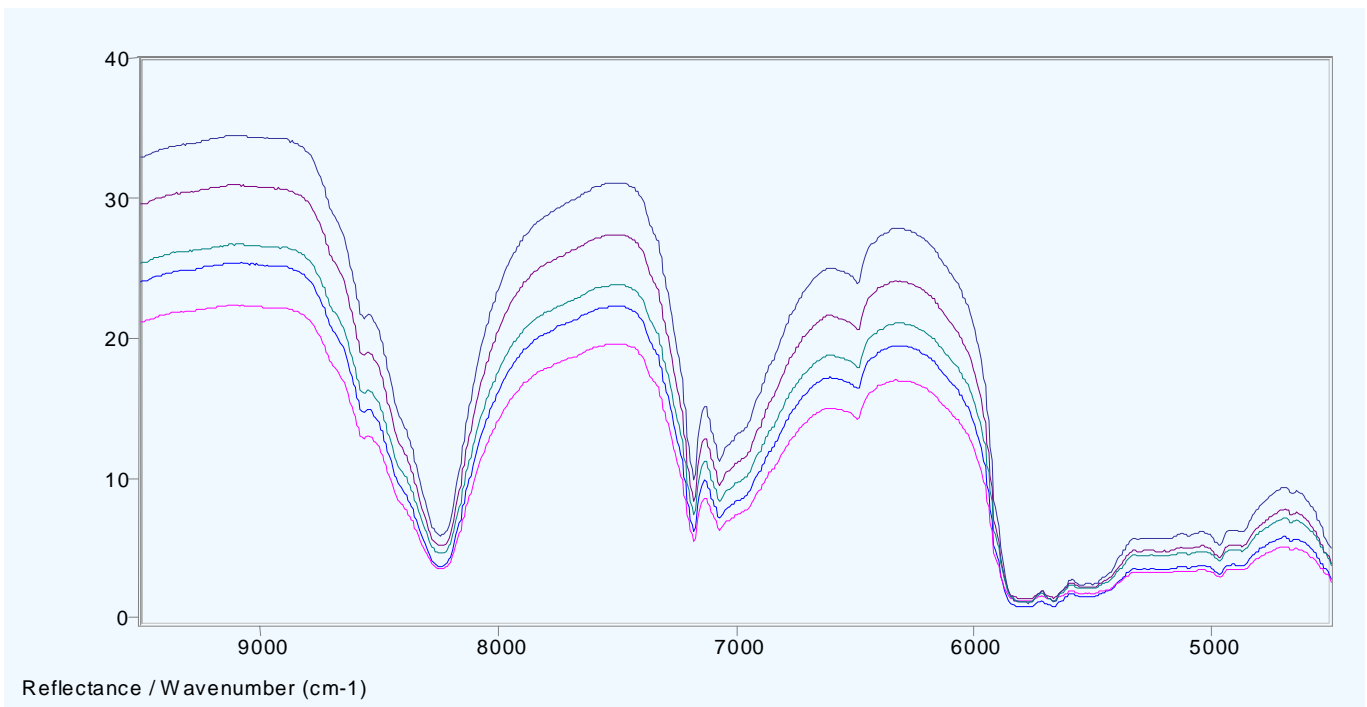


Figure 2: Spectra of five areas of a sample of 3 to 4 mm diameter polyethylene pellets obtained with a 10 mm spot diameter.

The uncertainty caused by limited viewing area relative to particle size can be reduced to some extent by applying a multiplicative correction to the raw data to partially correct for the lost signal and a subtractive correction to account for specular reflectance. Figures 3 consists of

overlaid second derivative, Kubelka-Munk transformed spectra corresponding to two of the spectra of Figure 2 after applying these corrections. Although the multiplicative and subtractive corrections do reduce the scatter between the spectra, the variations are still too great to be acceptable for many analyses.

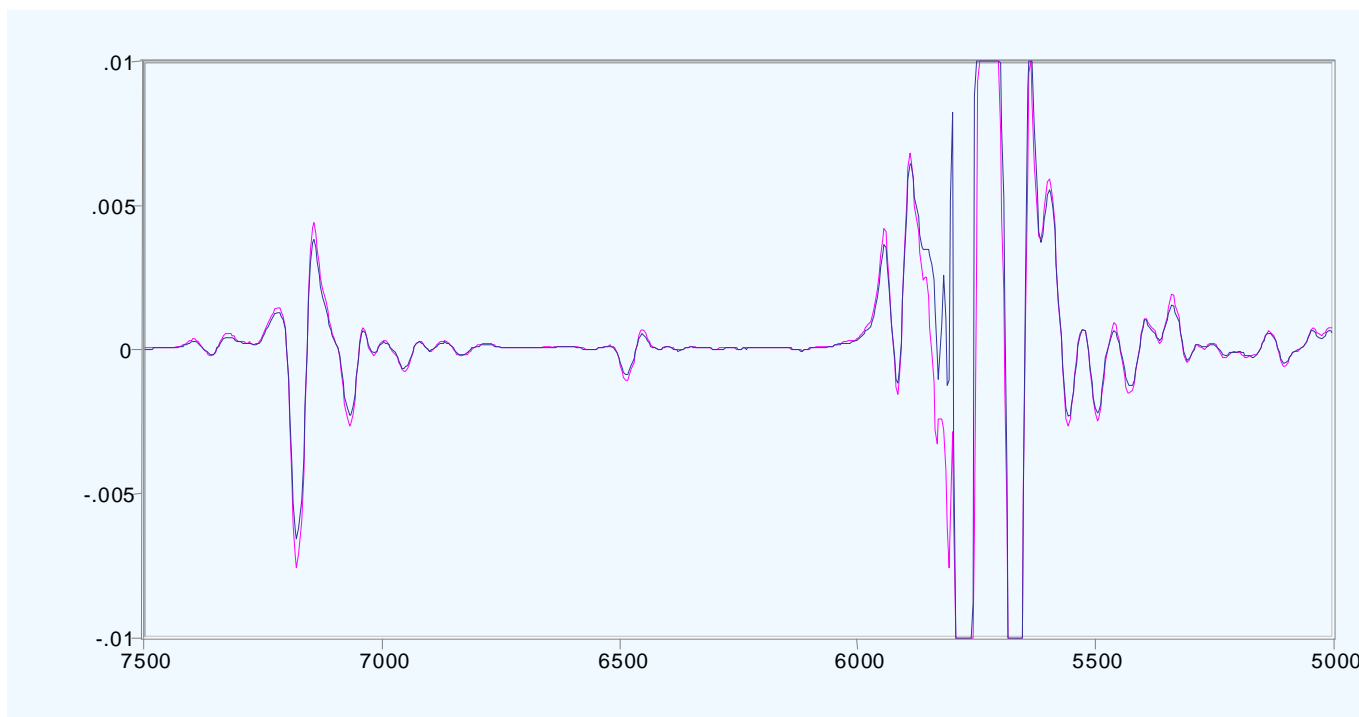
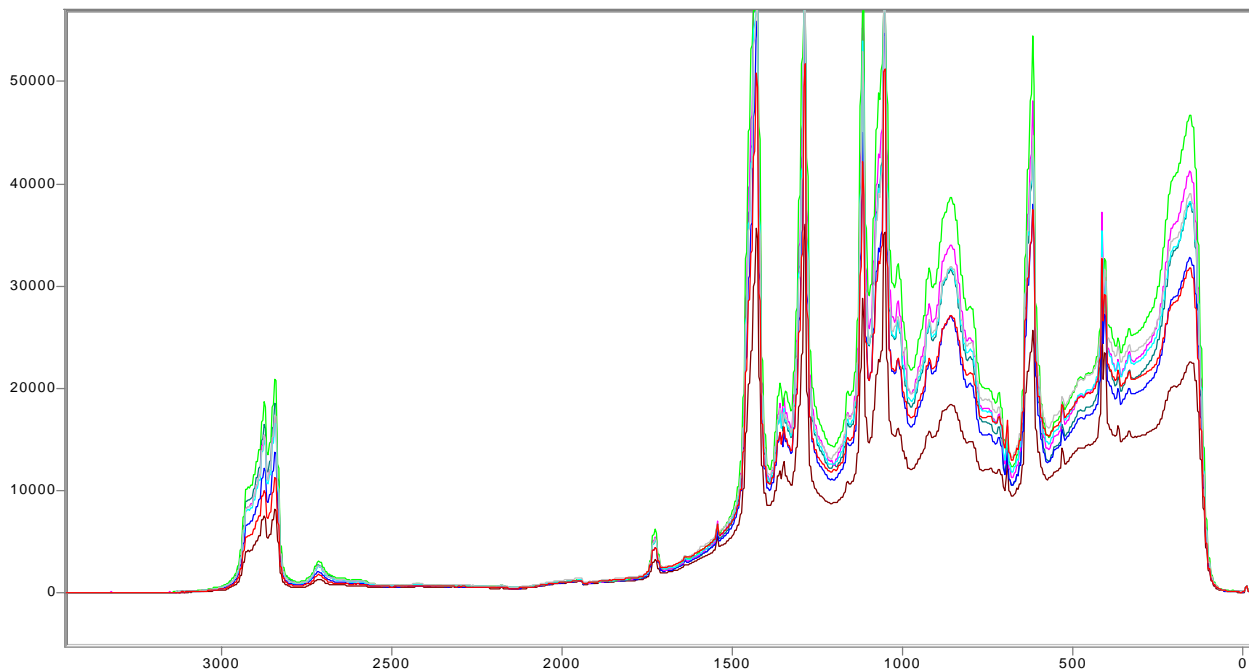


Figure 3: Second derivative, Kubelka-Munk spectra corresponding to two of the spectra of Figure 2 after performing multiplicative and additive corrections.

Figure 4 includes seven Raman spectra of a single 3 – 4 mm diameter polyethylene pellet viewed in seven random orientations. In this case, the viewed area (0.3 mm in diameter) was considerably smaller than the pellet. Once again, we see a substantial variation in overall signal level – probably due to variations in specular reflection and scattering losses and penetration depth. However, these variations do not alter the relative band heights or shapes. This can be seen by scaling the spectra to match at a given frequency and then taking the second derivative. The result is given in Figure 5. As can be seen, all of the spectra match very well with the exception of some spurious features in one spectrum – probably due to a small area of contamination.

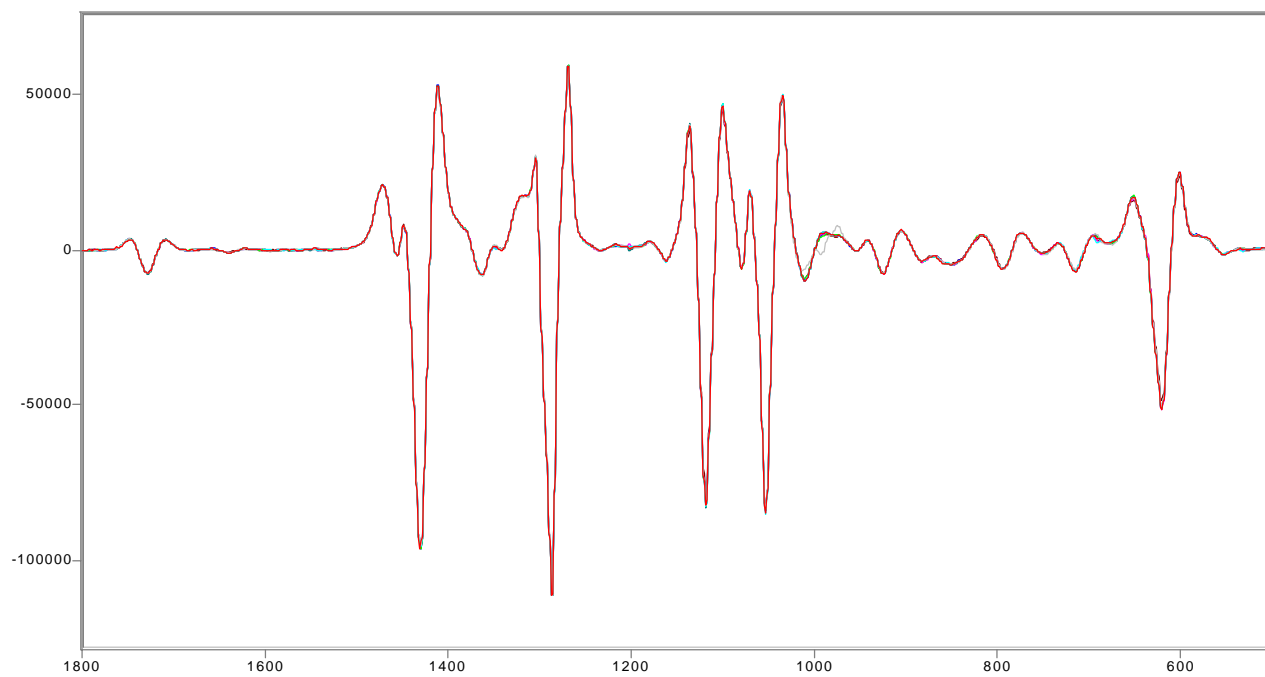
Comparing Figures 3 and 5, we find that Raman spectroscopy has yielded a much more repeatable result without requiring the signal level to be sacrificed by spreading the beam and without introducing the uncertainties in band shape caused by the corrections used in the diffuse reflectance case. In general, we can state that grain size and related form factors are much more of a problem for diffuse reflectance than for Raman spectroscopy.



Arbitrary Y / Raman Shift (cm-1)

Overlay X-Zoom SCROLL

Figure 4: Raman spectra of a 3-4 mm diameter polyethylene pellet in seven random orientations.



Derivatv / Raman Shift (cm-1)

Overlay X-Zoom SCROLL

Figure 5: Scaled second derivative spectra corresponding to the seven spectra of Figure 4.

Analysis of particulate matter in a liquid matrix:

One particular measurement task that was brought to us by a customer involved measuring the concentration of polymer particles being transported in a water slurry. We simulated this task by using the same 3 to 4 mm diameter polyethylene pellets used above. We first filled a glass beaker with the pellets and obtained a diffuse reflectance spectrum through the beaker wall. The result is shown as the upper trace in Figure 6. We next poured enough water into the beaker to just fill the space between the pellets without reducing the density of the pellets (lower trace).

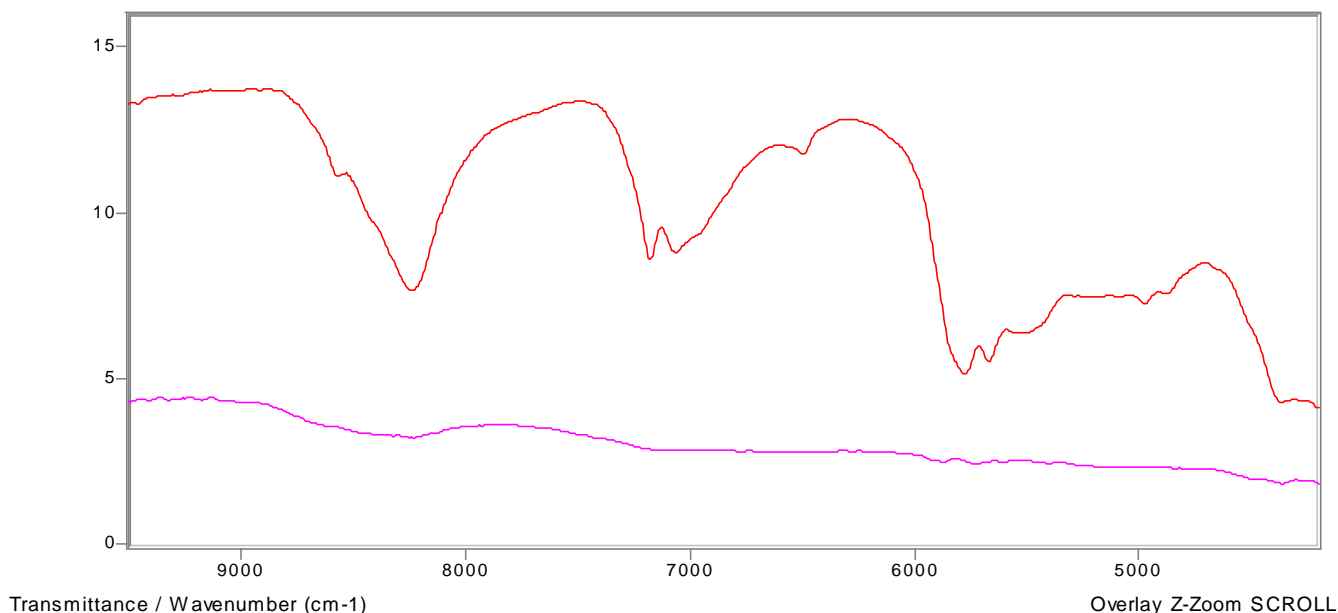


Figure 6: Diffuse reflectance spectra of 3-4 mm polyethylene beads through a beaker wall. Upper trace: dry; Lower trace: in a water matrix.

As Figure 6 illustrates, the diffuse reflectance spectrum of polyethylene almost disappears when the space between the pellets is filled with water. This is largely due to the fact that the diffuse reflectance, in this case, results from multiple specular reflections at the surface of the pellets. The refractive index of the water partially matches that of the pellets, greatly reducing the reflectance and allowing the light to penetrate further into the sample -- where it is eventually absorbed by the water or scattered out of the probe field of view. The residual background is largely due to reflection by the beaker.

Figure 7 includes time averaged Raman spectra of vigorously stirred mixtures of water and polyethylene pellets obtained with an RFP-480 process Raman probe immersed in the vessel. The concentrations ranged from zero to 11.3 %. To obtain a calibration for this data, we first took second derivatives of all of the spectra to minimize the effects of the fluorescence background and then used PCR. The result is shown in Figure 8.

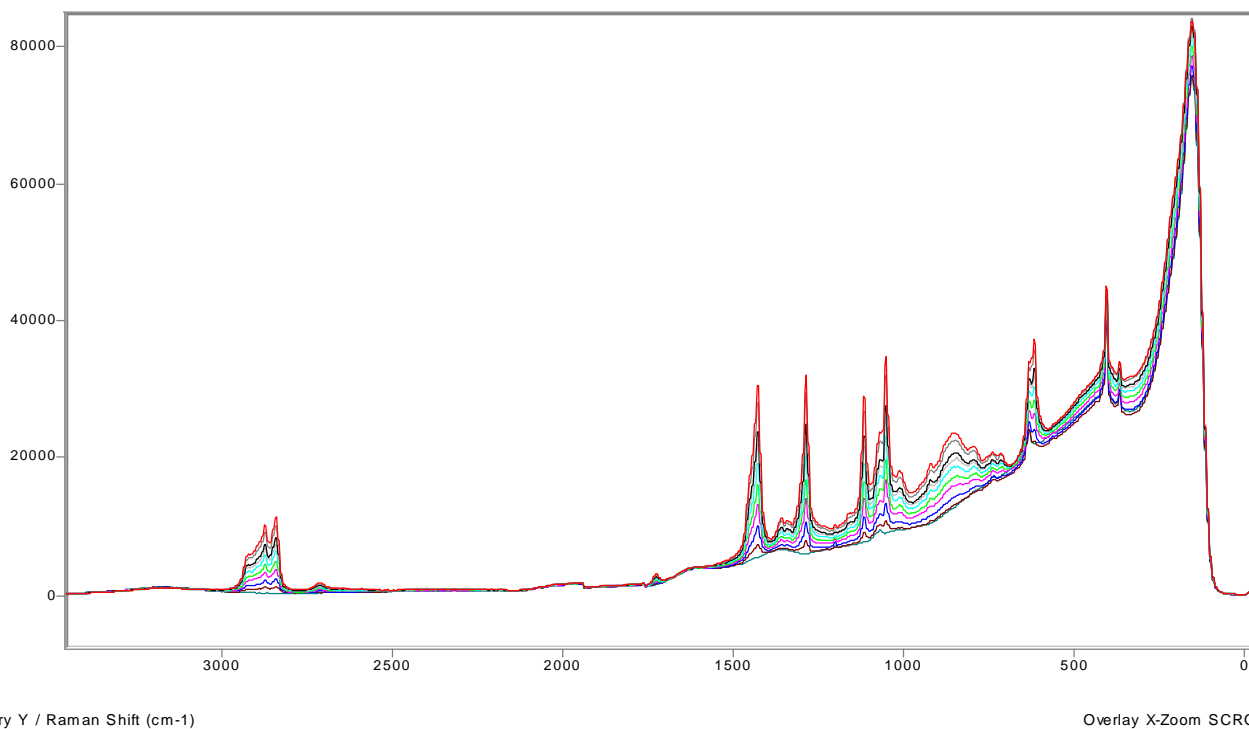


Figure 7: Raman spectra of polyethylene pellets in water at concentrations from zero to 11.3%.

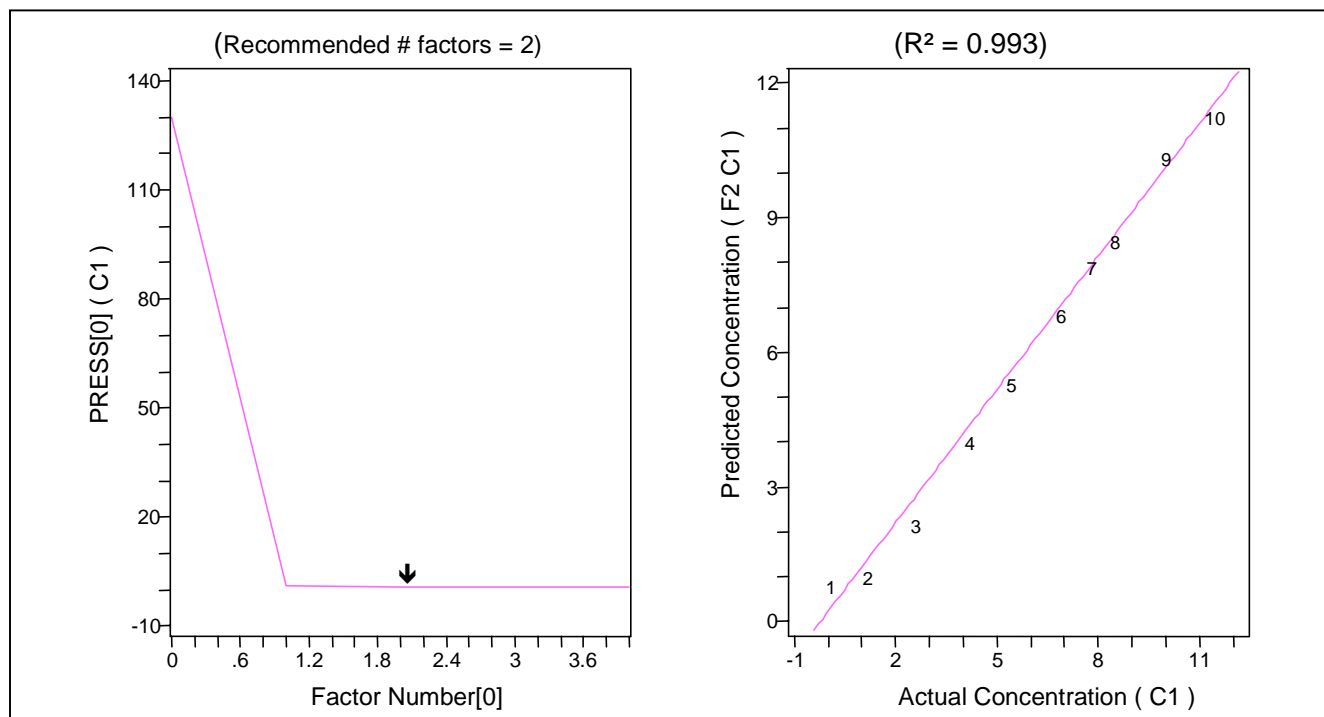


Figure 8: PCR calibration for polyethylene concentration in a water slurry.

As the two experiments above illustrate, Raman spectroscopy is a far better means for monitoring concentrations of polymers in water than near-IR diffuse reflectance. The power of Raman for this analysis is a result of two factors. First, water is a weak Raman scatterer, although it does have a band in the 1600 cm⁻¹ region that can be used for normalization.

Second the fact that the Raman signal is linear in concentration makes it possible to co-add rapidly varying raw signals on the fly. In this experiment, the signal level for individual scans actually varied between zero and 100% as individual particles passed through the probe's field of view.

Diluent effects:

As I have shown in an earlier paper, the Kubelka-Munk function will have a non-linear dependence on concentration if the sample system is a mixture of substances having different scattering coefficients (Ref. 1). For the simple case of an absorbing scatterer mixed with a non-absorbing diluent, the concentration dependence is given by the equation:

$$F(R) = aC/[bC + 1] \quad \text{where } a = k_1/s_2 \text{ and } b = s_1/s_2.$$

Here k_1 is the absorptivity and s_1 and s_2 are the scattering coefficients of the absorbing and non-absorbing species, respectively.

As a test of the predicted concentration dependence we acquired spectra of various absorbing powders diluted, in turn, by strongly scattering and weakly scattering diluents. A typical example is given in Figure 9 for niacin (a strong scatterer) diluted by KCl (a weak scatterer). This is a plot of the second derivative peak value of the band centered at 6028 cm^{-1} as a function of niacin concentration. The solid line is a fit of the equation given above to the data, using the values $a = 1.65$ and $b = 5.6$. After further experimentation, we concluded that the scatter in data is due to variations in packing density.

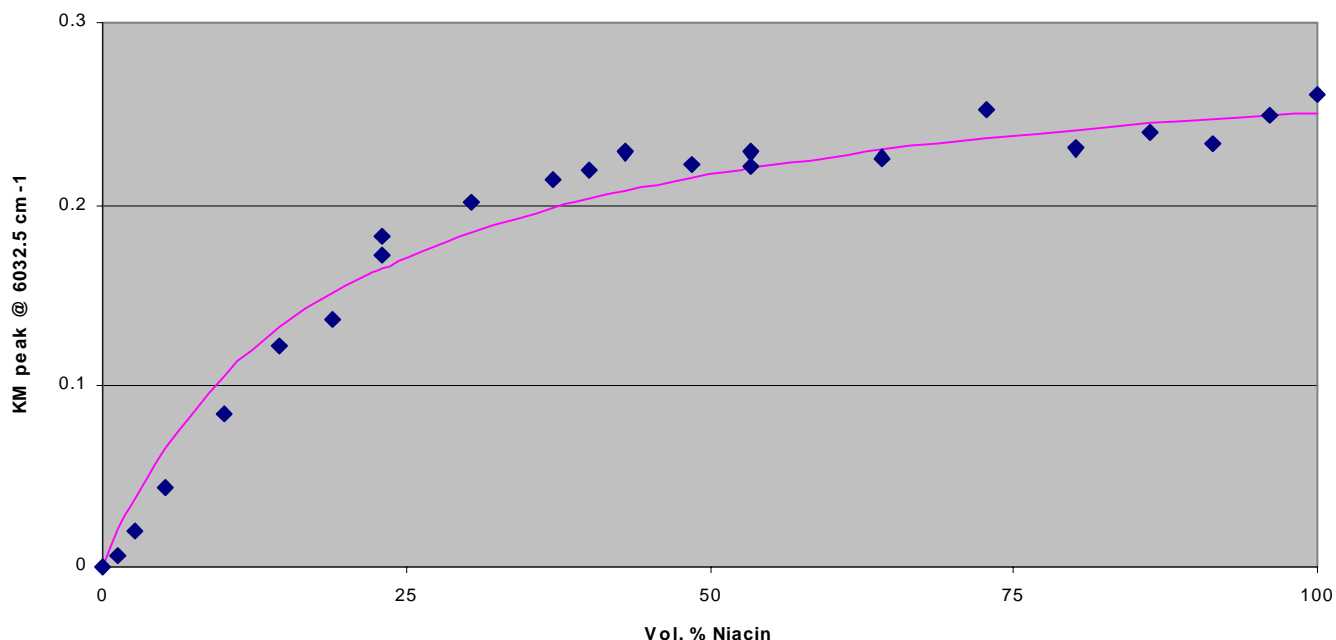


Figure 9: Theoretical fit to niacin/KCl Kubelka-Munk peak values.

We can draw two conclusions from Figure 9. First, it is possible to develop calibrations for non-linear diffuse reflectance data by fitting Kubelka-Munk intensities at specific frequencies to the appropriate theoretical curves. Second, for certain sets of conditions, the curve of Kubelka-Munk peak values versus concentration can be almost flat. In view of this fact,

combined with the unavoidable scatter in the data, it would be very difficult to use Kubelka-Munk measurements of predict concentration values under such conditions.

As a comparison, we obtained a set of Raman spectra for a similar set of niacin/KCl dilutions. The result is given in Figure 10. Once again, we have a non-linear dependence of the measured peak values on concentration. However, in this case, the inflection is in the opposite direction than the diffuse reflectance data and there appears to be less scatter. No fit is provided since we have not yet developed a theoretical prediction for the functionality. Never the less, with the aid of an appropriate normalization, data such as this could be used for calibration by performing a piecewise linearization or by developing an empirical non-linear fit.

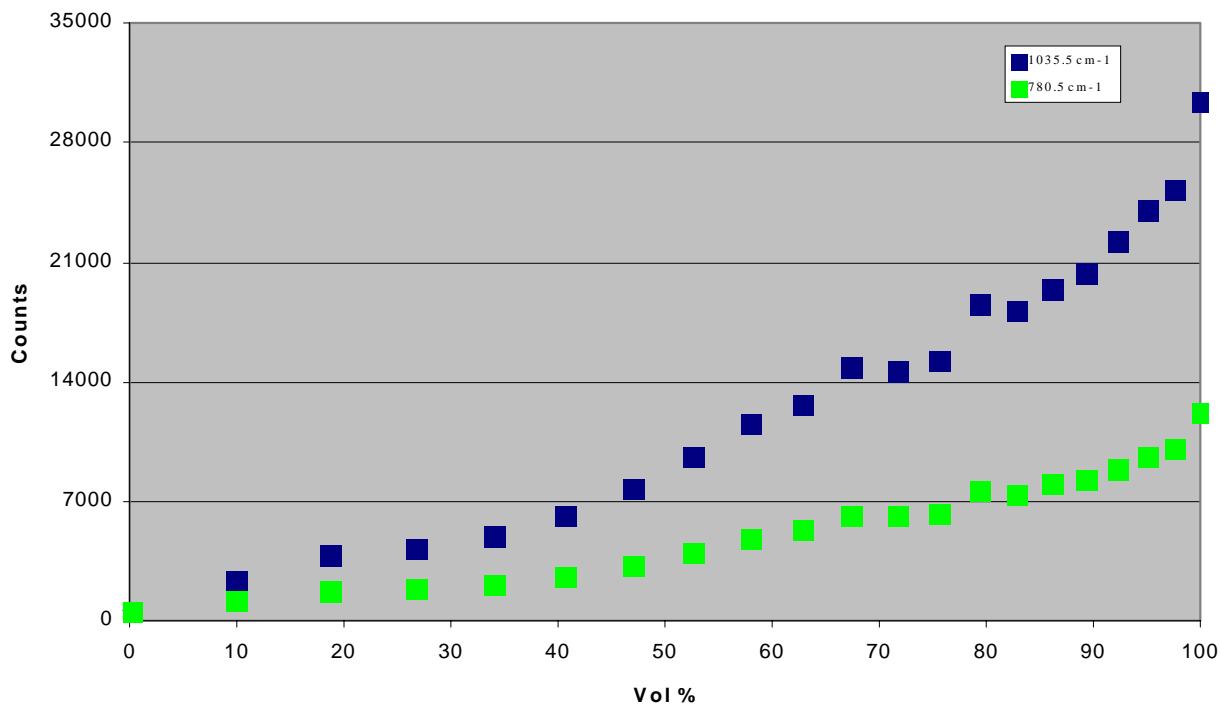


Figure 10: Raman peak height data for mixtures of niacin and KCl.

The difference in the functionality exhibited by Figures 9 and 10 can be understood as follows. In the case of diffuse reflectance, an increase in the scattering coefficient (as occurs with increased niacin concentration) leads to a reduction in penetration depth and hence in the interaction of the radiation with the sample. This, in turn, results in a reduction of the slope of the peak height vs. concentration curve. In the extreme case of $s_1 \gg s_2$, $F(R)$ becomes a constant and we have no information about concentration. The Raman case is different in that Raman scattering is an extremely rare event. As a result, any reduction in the intensity of the laser radiation due to Raman scattering is negligible. As long as the sample is transparent at the laser frequency, an increase in the scattering coefficient will result in a given photon experiencing more reflections and hence spending more time interacting with the sample before being scattered out of the probe's field of view. This results in an increase in the slope of the Raman signal vs. concentration plot with increased niacin concentration.

From the practicality viewpoint, a comparison of Figures 9 and 10 suggests that, for this particular example (a strongly scattering absorber diluted by a weak scatterer), Raman spectroscopy will provide generally more consistent data. However, for low concentrations, diffuse reflectance may have an advantage due to a stronger dependence on concentration in

this region. We should note, of course, that there is no practical way to internally normalize the Raman data when one of the constituents is inactive. In the case of diffuse reflectance, the need for normalization is mitigated by fitting the data to a theoretical nonlinear function.

Mixtures of particulate matter and active liquids:

Many current and potential applications of both Raman and near-IR spectroscopy involve slurries in which the properties of the liquid phase are to be monitored. In such cases, the solid phase may or may not be active. We will look at two examples, both employing TiO₂ as a convenient strong scatterer.

In the near-IR analysis of slurries involving an inorganic solid phase, most of the spectral features will be due to the organic liquid phase. The solid phase serves primarily as a scatterer. As shown in Reference 1, the predicted dependence of the Kubelka-Munk function on concentration in this case is

$$F(R) = (k/s)C_k/(1-C_k) \quad \text{Eq. 2}$$

Or
$$F(R) = (k/s)/(1-C_s)/ C_s \quad \text{Eq. 3}$$

Where k is the absorptivity of the clear liquid phase
 s is the scattering coefficient of the inactive solid phase
 C_k is the concentration of the liquid phase, and
 C_s is the concentration of the solid phase.

As an illustration of the behavior of this type of slurry in the near-IR, we studied stirred mixtures of TiO₂, water, and methanol. We first acquired diffuse reflectance spectra of mixtures of water and TiO₂ as a function of TiO₂ concentration. The experimental points in Figure 11 are measurements of the Kubelka-Munk peak heights of a water band as a function of TiO₂ concentration. The theoretical curve is a fit of Equation 3 to this data.

To test the potential for analyzing mixtures of organics in the presence of a scattering inorganic, we studied mixtures of water and methanol with the TiO₂ concentration maintained at 1%. Representative spectra are given in Figure 12, and the result of a PLS calibration is given in Figure 13.

It should be noted that any variation in the concentration of the scatterer will result in an error in the measurement of the active substances unless either the concentration of the scatterer is included in the calibration or an appropriate normalization is performed. Since the dependence on scatterer concentration is highly nonlinear, it would be difficult to obtain a calibration by using any of the linear regression methods. However, as I will illustrate below, it is possible to circumvent this problem by using an appropriate method of normalization.

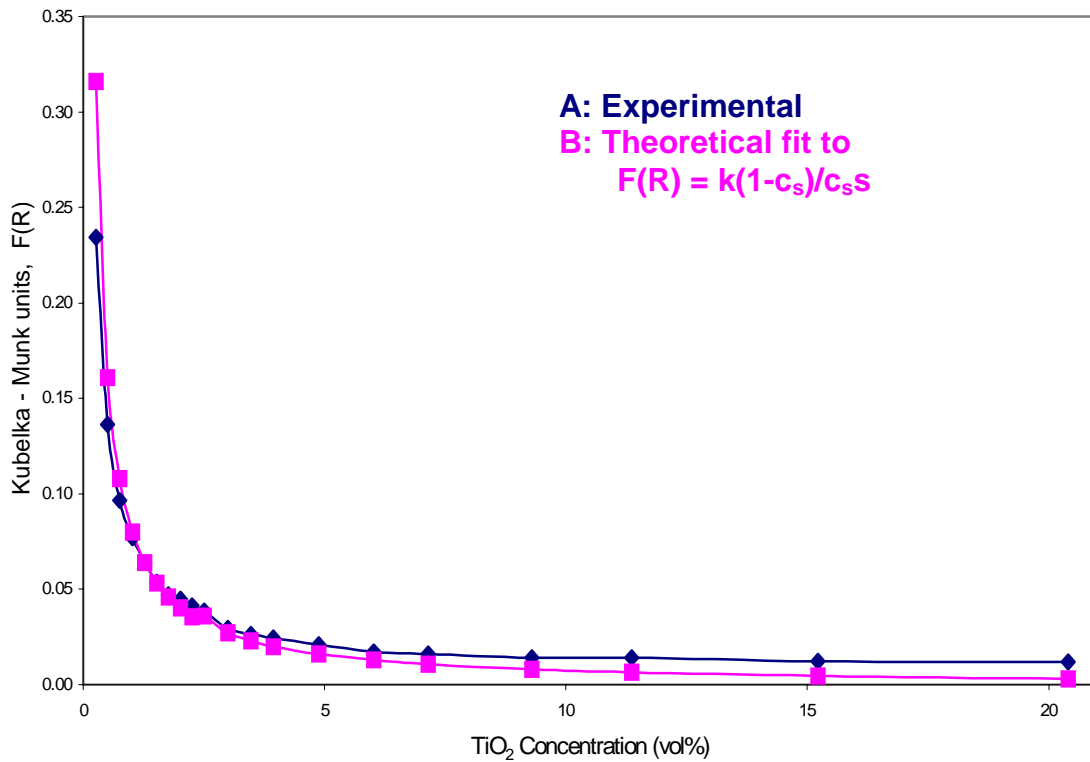


Figure 11: Plots of the measured and theoretical Kubelka-Munk values of the water band at 6906 cm^{-1} as a function of TiO_2 concentration.

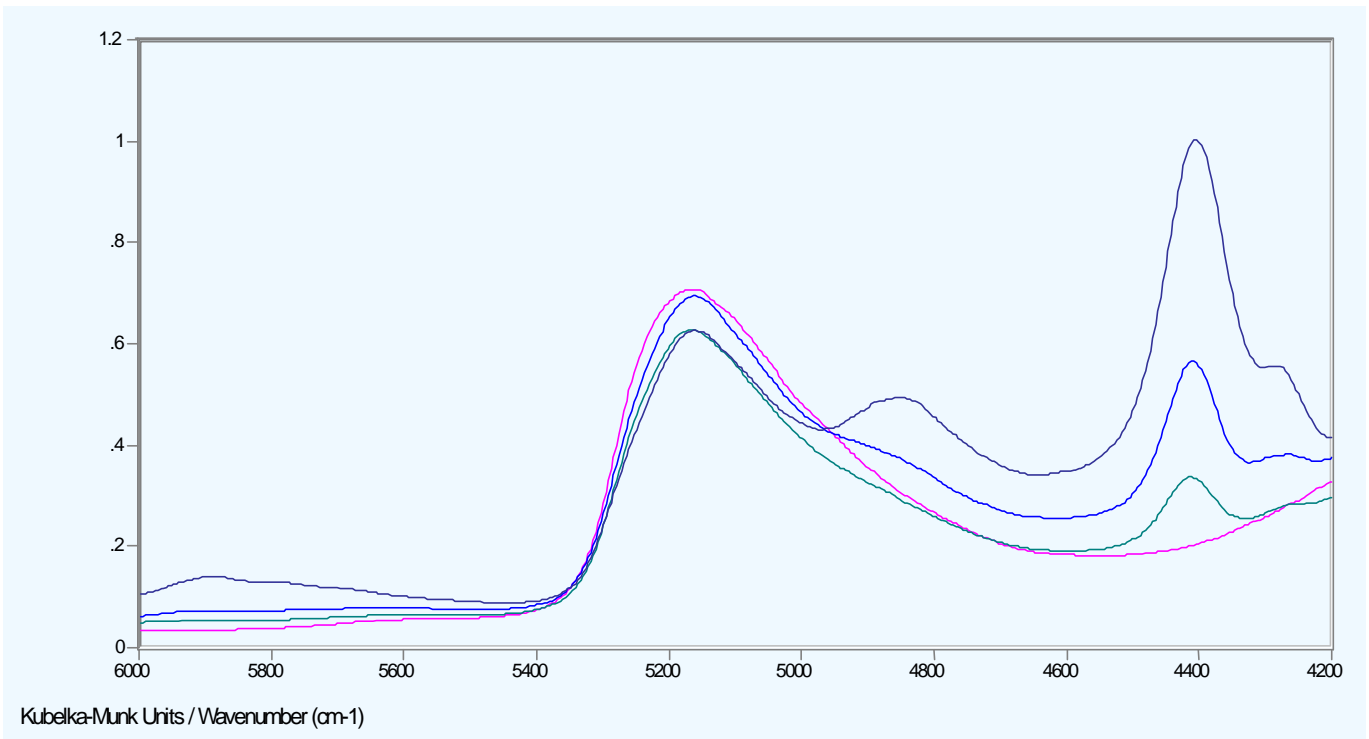


Figure 12: Kubelka-Munk transformed spectra of four mixtures of methanol and water with a fixed concentration of 1% TiO_2 powder.

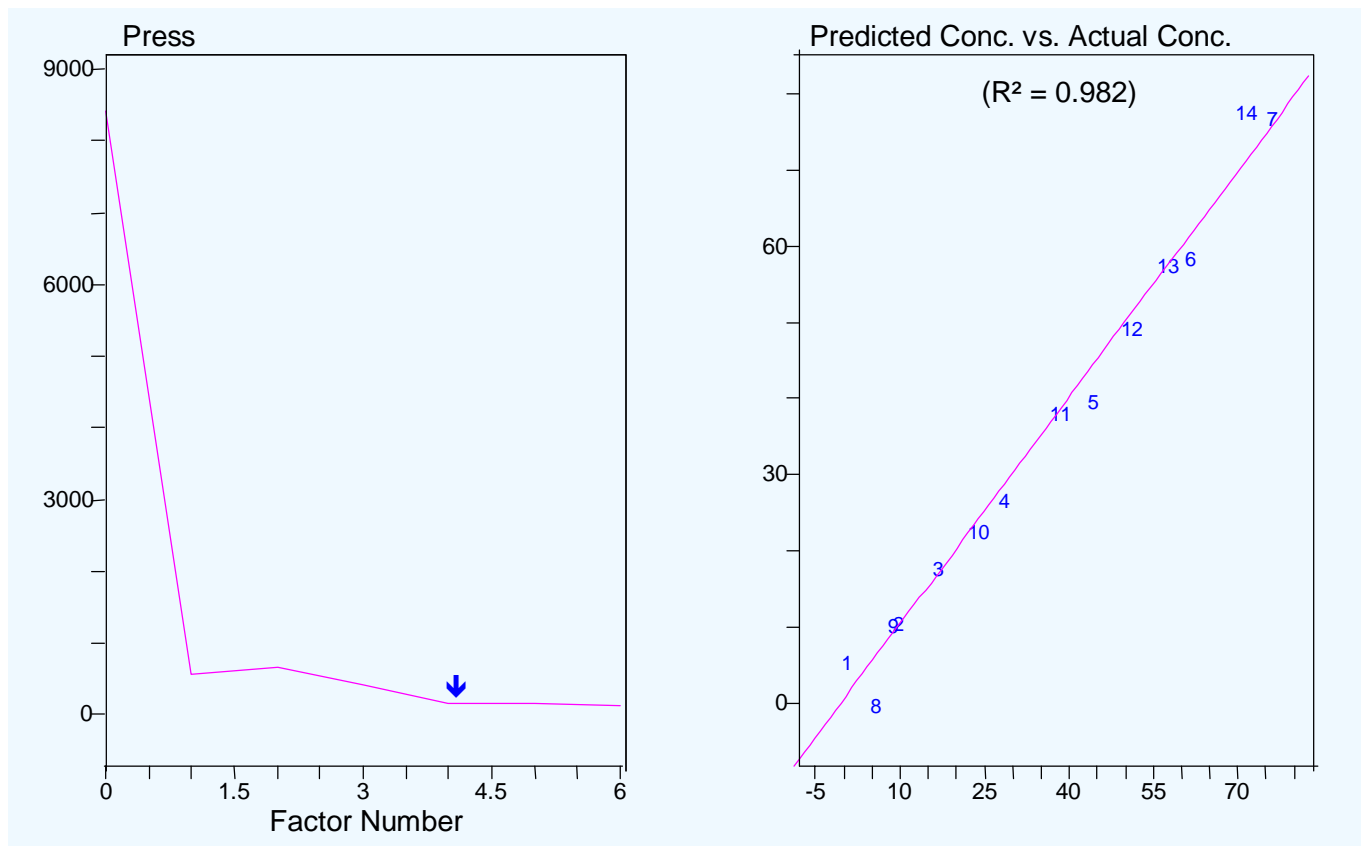


Figure 13: PLS analysis of of mixtures of methanol and water in the presence of 1% TiO₂.

A major difference between the application of Raman spectroscopy and near-IR spectroscopy to mixtures of organic liquids and inorganic solids results from the fact that the inorganics will often have very strong Raman spectra. To examine this and the other factors relating to the Raman analysis of slurries, we studied stirred mixtures of TiO₂ and isopropanol. A comparison of the spectra of the two pure substances is given in Figures 14 and 15. We see that, although Isopropanol is a fairly strong Raman scatterer for an organic, the main TiO₂ peaks are almost two orders of magnitude stronger. Despite the disparity in the strengths of the bands, it is possible to develop a calibration for concentrations of mixtures of these two substances. To do this, we first took the second derivative of each spectrum. This greatly reduced the overlap between the spectra by discriminating against the broad features. We next recorded the signal values at the frequencies corresponding to the strongest peaks of the two substances as a function of concentration. The results are given in Figures 16 and 17.

Examining Figure 16 first, we see that the intensity at the frequency corresponding to the peak of the TiO₂ spectrum increases monotonically with TiO₂ concentration. The situation is substantially different, however, at the frequency corresponding to the isopropanol peak. In the absence of TiO₂ we see the very strong peak corresponding to pure isopropanol. With the addition of TiO₂ at a concentration of only 0.2%, the intensity drops more than an order of magnitude. With the addition of a few percent TiO₂, the intensity of this band increases by a factor of five or so. Above this it appears to have little concentration dependence.

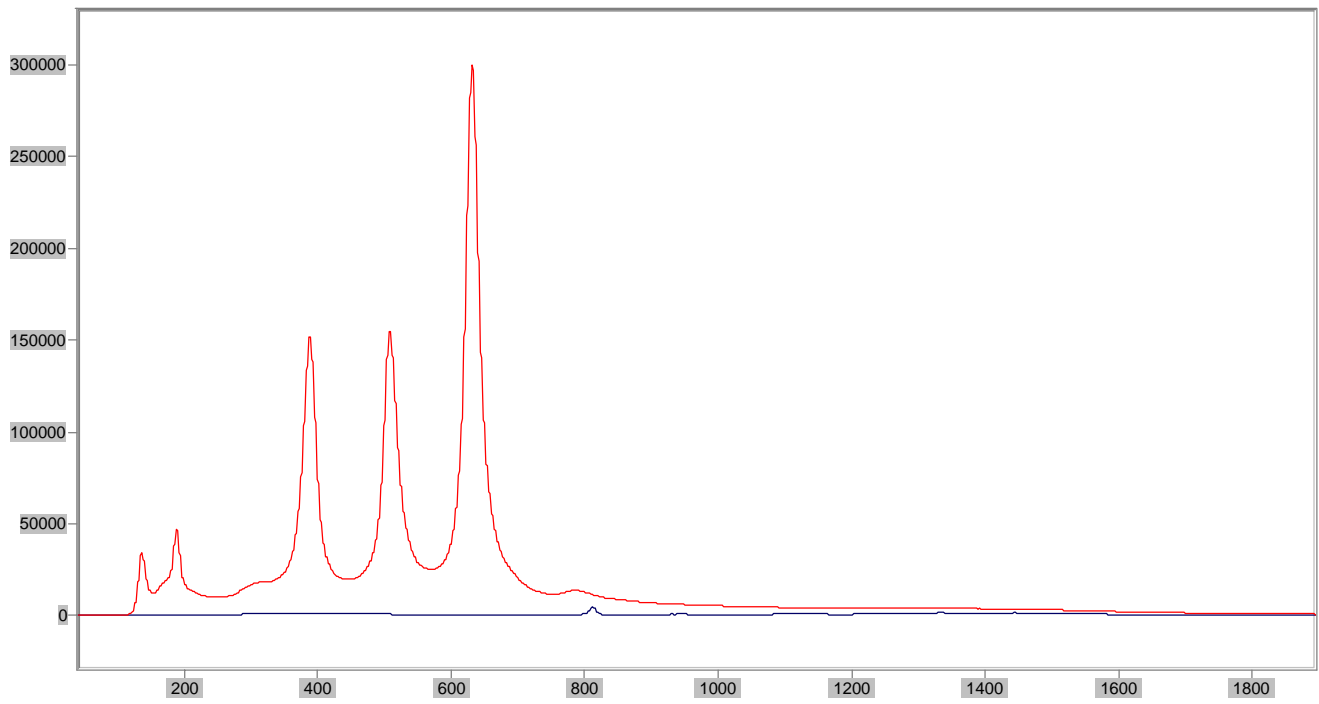


Figure 14: Raman spectra of TiO2 (upper trace) and isopropanol (lower trace).

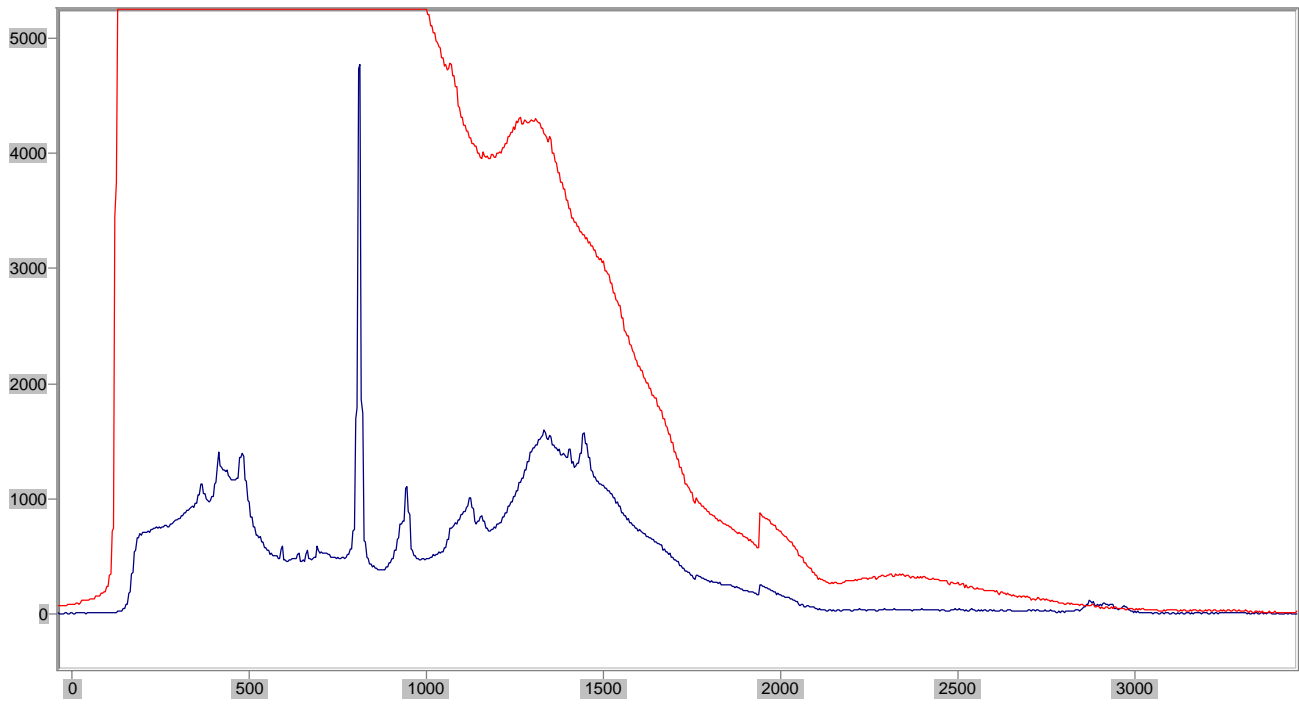


Figure 15: The spectral of Figure 14 expanded approximately sixty times.

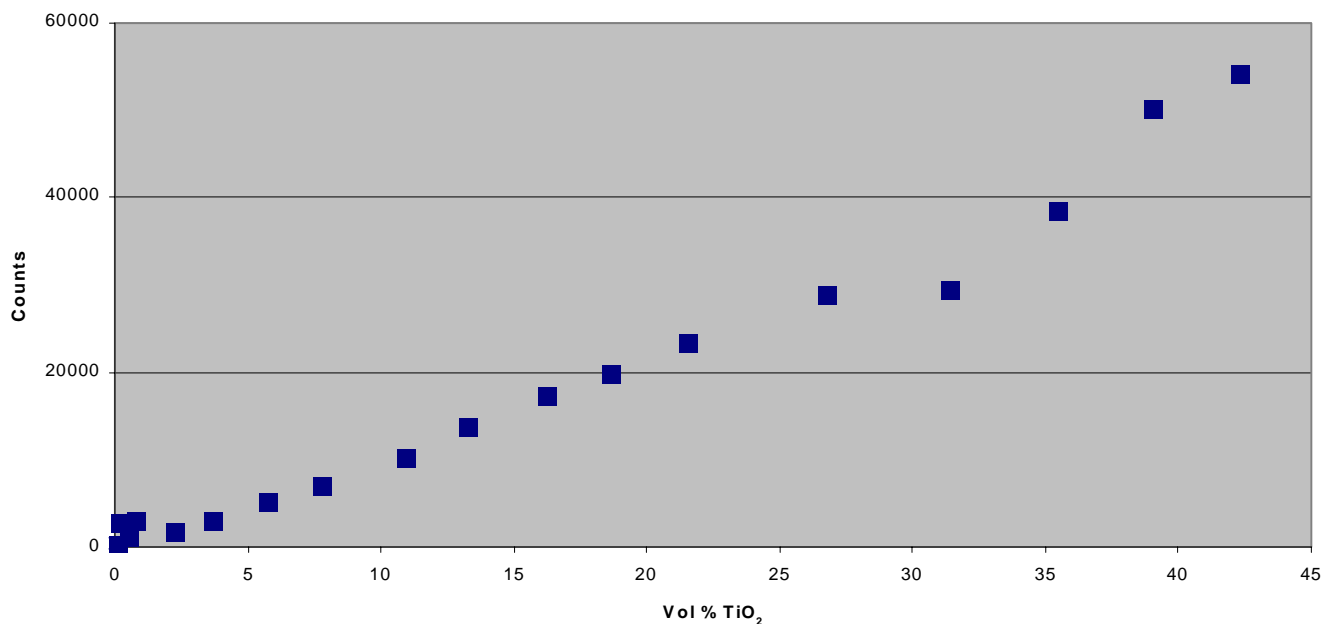


Figure 16: Second derivative peak height values of the TiO₂ band at 632 cm⁻¹ for mixtures of TiO₂ and isopropanol.

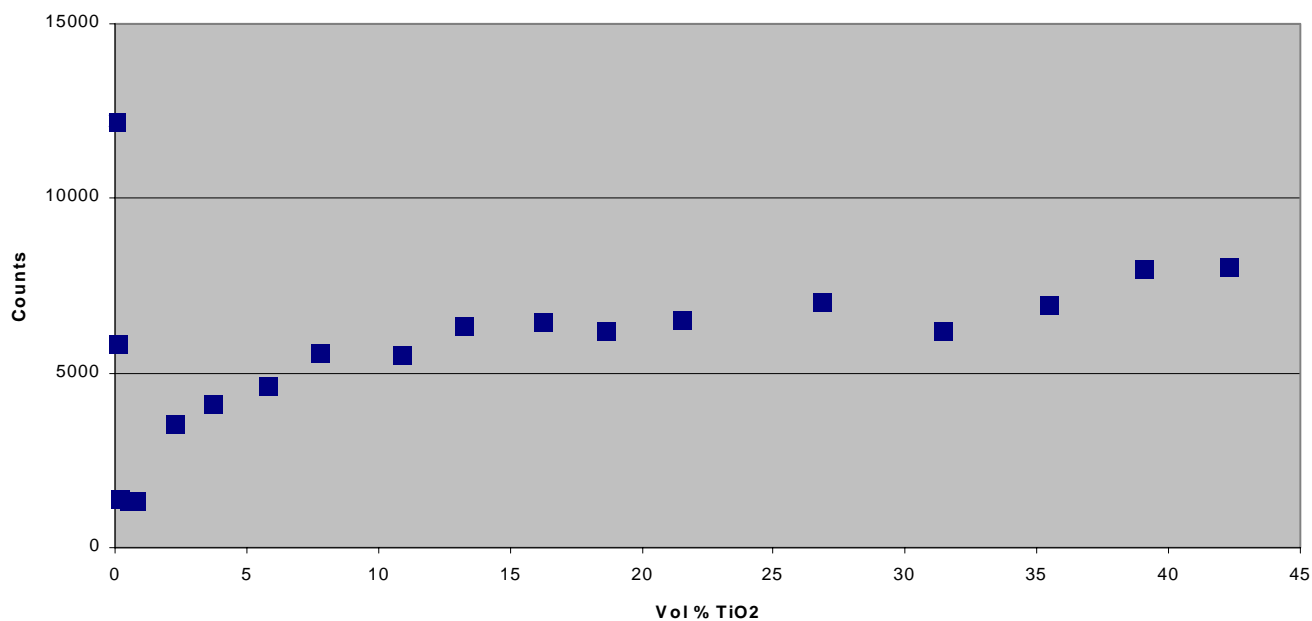


Figure 17: Second derivative peak height values of the isopropanol band at 811 cm⁻¹ for mixtures of TiO₂ and isopropanol.

The strange behavior of the isopropanol peak height is a result of the interaction of the various factors that determine the level of received Raman scattering. It can be understood at least qualitatively by the following simplistic analysis. First, the total Raman signal generated is determined by the number of interactions that take place between the laser beam and isopropanol molecules within the field of view of the receiving optics. Second, this signal can be reduced by diffuse scattering – of both the laser beam and the Raman signal – to the extent that light is scattered out of the probe’s field of view. Third, under certain conditions the signal can

increase if scattering results in a given photon traveling a greater distance before leaving the field of view.

The large signal obtained in the absence of scatterers, is partly the result of the substantial depth of field of the Raman probe (> 1 mm). The addition of even a very small amount of TiO_2 greatly reduces the penetration of the laser beam into the sample and at the same time scatters a portion of both the laser radiation and the Raman signal out of the field of view of the receiving optics. This results in the observed large drop in signal. With a further increase in TiO_2 concentration, the diffusion distance for scattered light decreases to less than the field of view of the probe (0.3 mm). In this domain, a given laser photon may experience several reflections before being scattered out of the field of view. This results in an increase in the number of potential observable interactions between the photon and isopropanol molecules and hence in the Raman signal. At still higher concentrations of TiO_2 the decrease in the actual concentration of isopropanol tends to offset further increases due to increased photon residence time within the field of view, and the signal levels out.

Calibrating heterogeneous mixtures:

The two examples given in the previous section illustrate the fact that, for both diffuse reflectance and Raman spectroscopy of heterogeneous mixtures, the relationship between concentration and spectral intensities can be highly nonlinear, and possibly even non-monotonic. This makes it very difficult to apply multivariate techniques involving linear regression, unless the analysis is restricted to a narrow range of concentrations (Ref. 3). A second issue for both of these forms of spectroscopy is that, since they do not obey Beer's law, they require some sort of normalization to remove overall signal level uncertainty. I will address both of these issues here for the simple case of band strength analysis.

In this section, I will give some examples which illustrate the fact that, in many cases, both non-linearity and signal level uncertainty can be handled by appropriate normalization. Let's first consider Raman analysis. In the case of simple chemical reactions in which some features of the spectrum are unaffected by the reaction, the normalization problem is typically solved by ratioing a changing reaction dependent band against a constant band, i.e.

$$C_1 = k_1 S_1 / S_2 \quad \text{Eq. 4}$$

where S_1 and S_2 are the heights of the changing and fixed bands and k_1 is a calibration coefficient.

In a blending application, there are no constant bands. Furthermore, as we've seen above, the band strengths can be strongly affected by differences in the diffuse scattering characteristics of the components. However, we do have two very useful pieces of information at our disposal. First, we know that the sum of all component concentrations is equal to one. Secondly, we know that the Raman signal of each chemical species is affected in the same way by diffuse scattering. In developing the equations given below, I have used these facts as well as the simplifying assumption that the diffuse scattering effect is the same for each of the bands being employed, i.e. that it is independent of frequency across the range of the Raman shifts of interest.

Requiring that the sum of all components is equal to one is an example of “normalization by closure” (Ref. 4). In principle, it should be possible to employ this normalization for any number of components by simply requiring:

$$\sum_i C_i = 1. \tag{Eq. 5}$$

For the case of two component blending, this requirement reduces to

$$C_i = [k_{ij}S_i - k_{ji}S_j] / [(k_{ii} - k_{ij})S_j + (k_{jj} - k_{ji})S_i] \tag{Eq. 6}$$

where i and j can each take on the values 1 and 2, S_1 and S_2 are measured band strengths, C_1 and C_2 are the concentrations, and the k’s are calibration constants.

By imposing the closure requirement, we have developed expressions for the concentration values which are independent of factors – such as concentration dependent diffuse scattering – which can distort the raw data. For each measured spectrum, we will have two equations of this form, one for each component. Thus, given the measurement of two or more spectra corresponding to known concentrations, we can solve for the four “k” values and develop a calibration which is valid for any spectrum of an unknown mixture of these species. As an initial test of this approach, I applied it to the TiO_2 /isopropanol data reported in the previous section. The results are given in Figure 18.

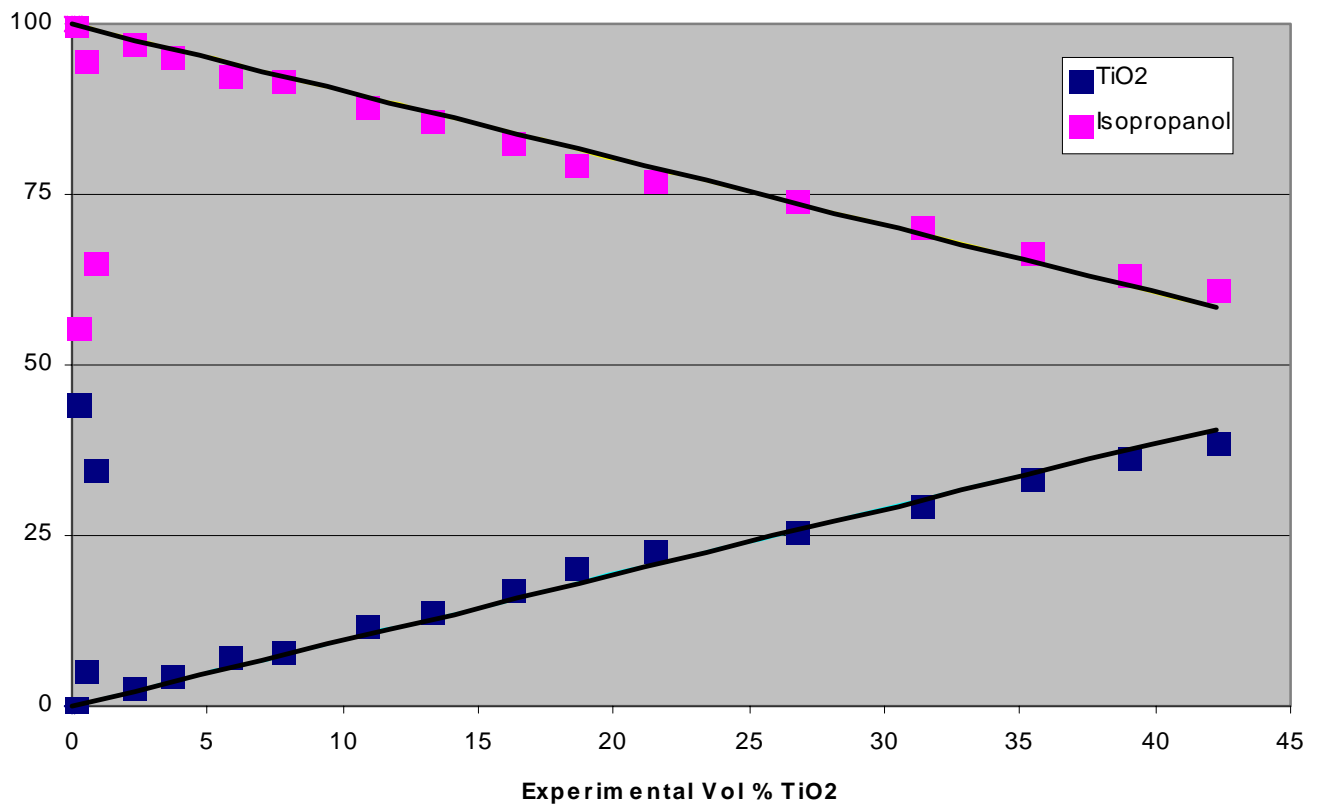


Figure 18: TiO_2 and isopropanol concentration calibration derived from the data of Figures 16 and 17 by requiring that the sum of the components is equal to 100%.

Aside from two pairs of outliers corresponding to very low concentrations of TiO₂, this approach has produced a linear plot of measured versus predicted concentration. The normalized data also appears to have less scatter than the raw data.

As a final example, we studied mixtures of niacin (a strong scatterer) and ascorbic acid (a weak scatterer) by both Raman and diffuse reflectance. A linear fit to the Raman data, using closure normalization, is given in Figure 19. As in the previous example, the normalization step produces a much more linear dependence on concentration than exhibited by the raw band strength data.

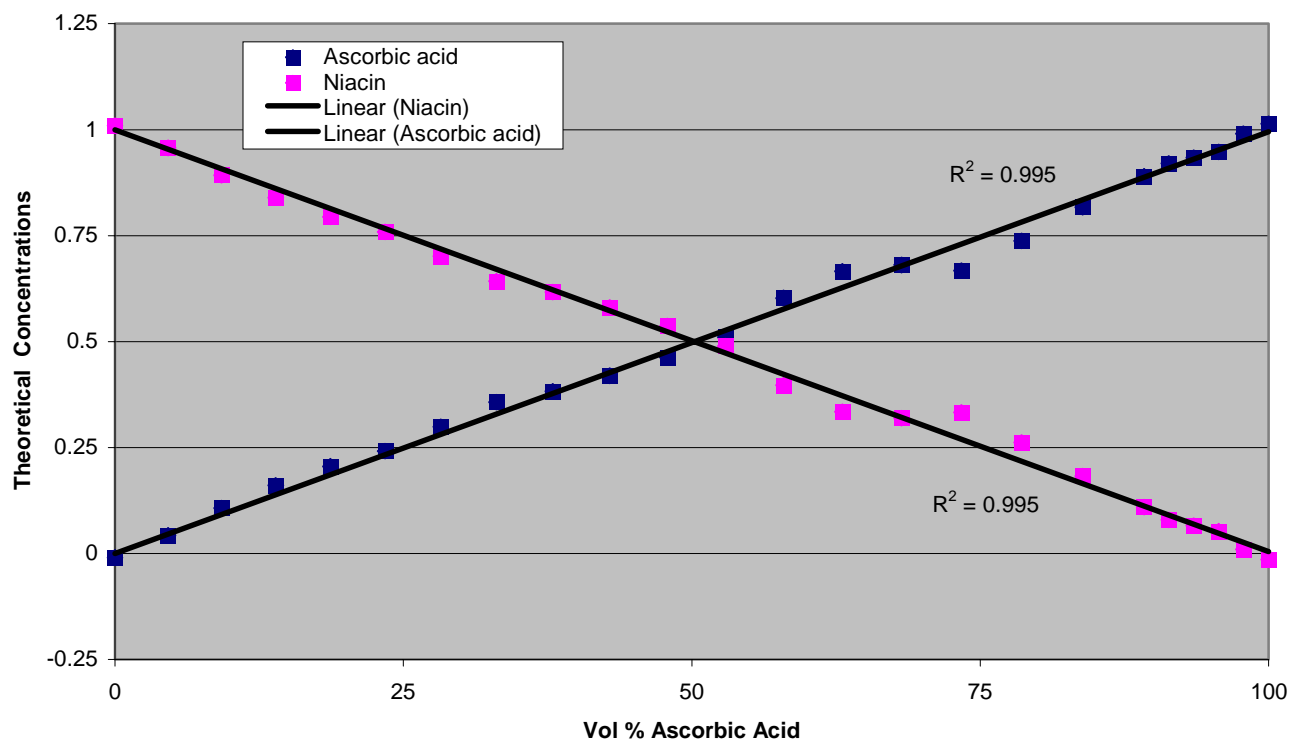


Figure 19: Predicted versus known concentrations of mixtures of ascorbic acid and niacin obtained from second derivative Raman peak height data by using closure normalization.

For the diffuse reflectance comparison, we first collected spectra of mixtures of ascorbic acid and niacin over the full concentration range, ratioed against a white Spectralon™ target. We next converted each of these to the Kubelka-Munk format and calculated the second derivative spectrum. Using this set of data, we tried two different approaches to data reduction.

For the first approach, we simply performed a full spectrum PLS calibration. The results are given in Figure 20.

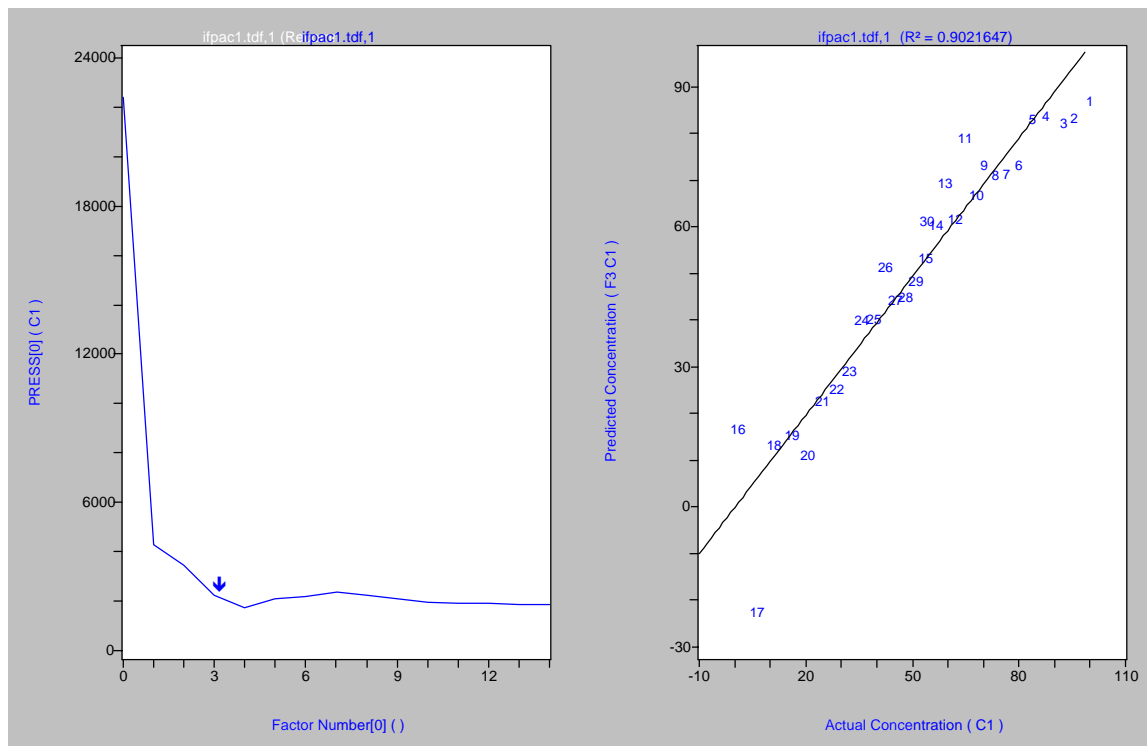


Figure 20: PLS calibration for ascorbic acid, mixed with niacin, based on second derivative, Kubelka-Munk, diffuse reflectance data.

Our second approach to calibration, was similar to that used for the Raman data. We first, plotted the second derivative peak heights at the frequencies corresponding to the strongest bands of both substances. The result is given in Figure 21. As in the case of the dilution of niacin by KCl, this data shows both marked non-linearity and substantial scatter.

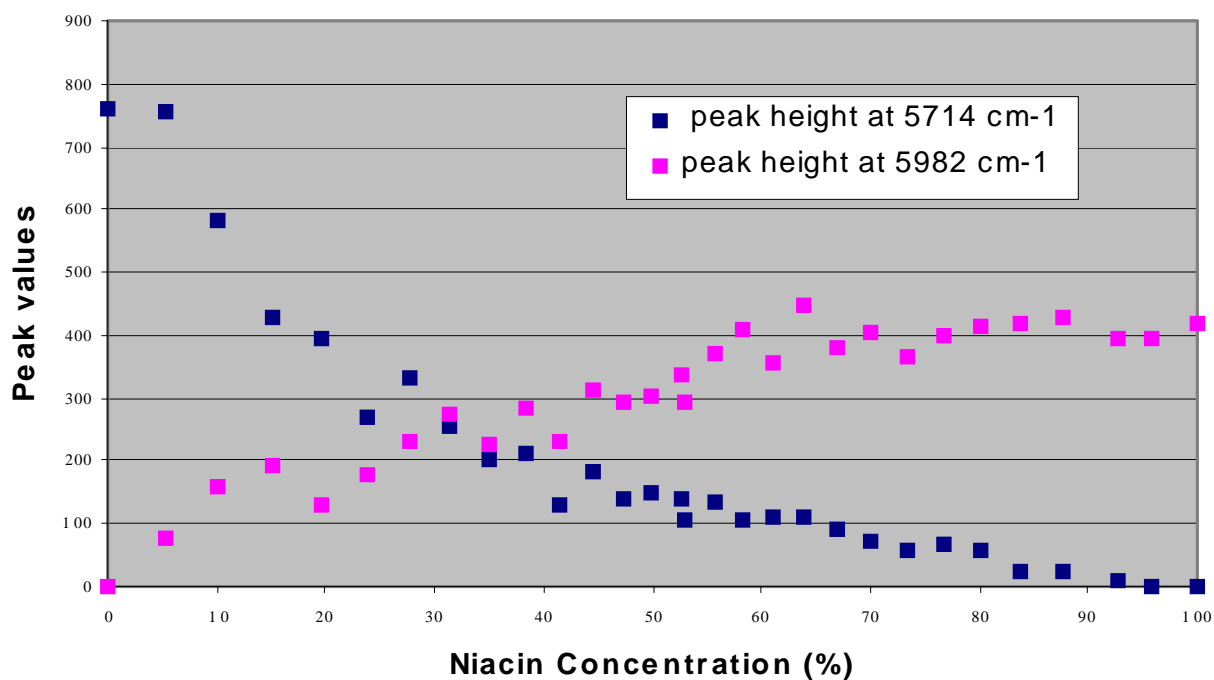


Figure 21: Second derivative Kubelka-Munk peak heights for mixtures of ascorbic acid and niacin.

We next normalized this data by using the same approach as we applied above for Raman analysis. However, in this case we placed the closure requirement on the Kubelka-Munk peak values rather on the concentration. We have established theoretically that, at least for a two-component system, once the K-M peak values are properly normalized, the concentration values will also be normalized. This is an interesting result in view of the non-linear relationship between the Kubelka-Munk function and concentration. The result is shown in Figure 21 along with a fit to the theoretical relationship between the Kubelka-Munk function and concentration.

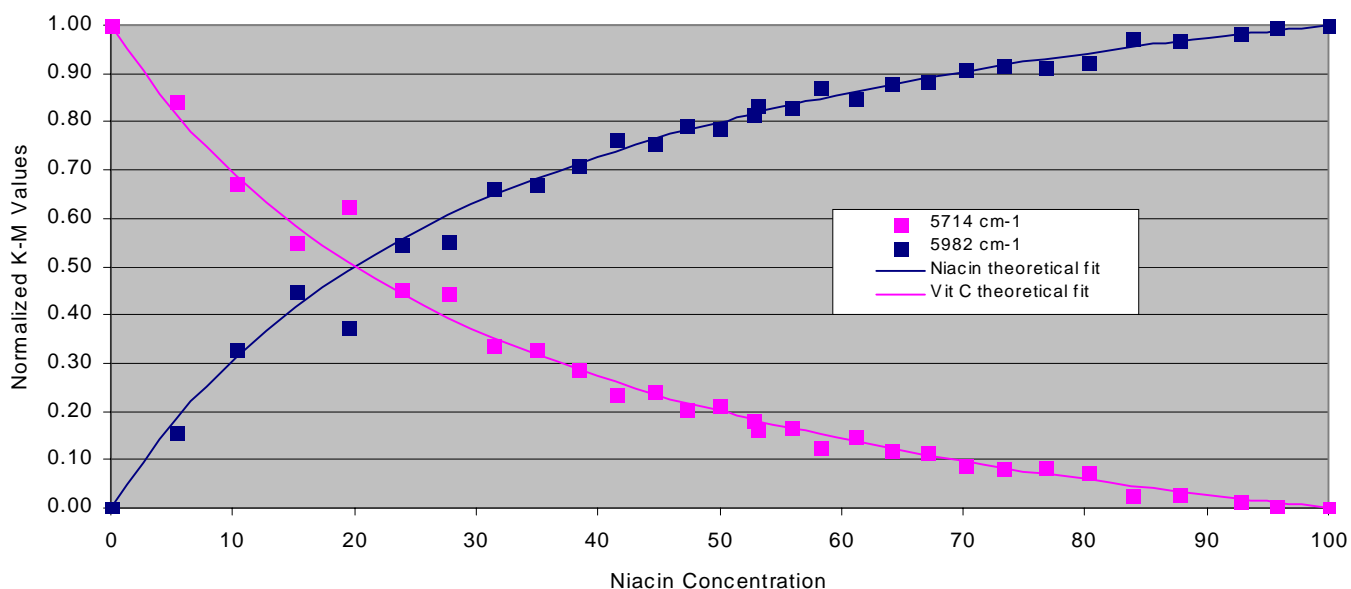


Figure 22: Second derivative Kubelka-Munk peak heights corresponding to the data of Figure 21 after closure normalization.

This result is interesting in that the closure normalization has resulted in a set of values which not only fit the expected functionality – with the exception of one pair of outliers – but also exhibit much less scatter than the raw peak height data. However, this result is not at all surprising since we know that much of the scatter in the data is due to packing density variations, and these should be common to both components.

It is enlightening to compare Figure 22 with the PLS calibration illustrated in Figure 20. Clearly, fitting the normalized data to a theoretical non-linear curve results in a far better calibration than the linear regression approach. In fact, the points that were furthest from the regression line (points 16, 17, 20, 26, 13, and 11) fall very close to the non-linear fit, while the pair of outliers at 20% niacin (point # 5 of Figure 20) is a good fit to the regression line.

CONCLUSIONS:

I have already stated a number of conclusions as they related to the individual experiments reported above. The more important of these are summarized in outline form in Table I, below.

Topic	Diffuse Reflectance	Raman
Pretreatment	Kubelka Munk	None needed
Granularity	Problematic	OK
Water matrix	Problematic	OK
Slurries	OK	OK
Inactive diluant	Curve fitting required	Quant. Problematic
Heterogenous mixtures	Curve fitting required	Unity sum normalization allows quantification
Density variation effects	Mitigated by normalization	Eliminated by normalization
Broad spectrum chemometrics	Not applicable in many cases	Applicable but seldom needed

TABLE I: Summary of specific conclusions related to particular sample characteristics.

Generalizing, we can state that near-IR spectroscopy has the advantage of mature hardware, lower cost of ownership, and insensitivity to various factors such as fluorescence, pigmentation, and background illumination that can degrade Raman performance. In addition, near-IR transmission has the advantage of adherence to Beer's law with the result that multiplicative errors can be ignored. Compared to near-IR diffuse reflectance, Raman spectroscopy has the advantage of greater specificity and, when compared to near-IR diffuse reflectance, generally greater accuracy for both quantitative and qualitative analysis.

Near-IR diffuse reflectance and Raman spectroscopy have some characteristics in common. In particular, since neither obeys Beer's law, they both require some sort of normalization to separate multiplicative errors from true concentration dependence. And both can exhibit highly non-linear concentration dependence for heterogeneous mixtures. In addition, diffuse reflectance spectra were found to be highly dependent on packing density of the samples.

In order to normalize the analysis of mixtures of active substances, I have imposed the requirement that the sum of the measured concentrations be equal to one. In the case of diffuse reflectance, this requirement can be met by normalizing the sum of the calculated peak values of the Kubelka-Munk function for each substance to one. For the cases studied, this approach has been found to provide the following benefits: It obviated the need for an absolute intensity reference. It corrected non-linearity caused by dissimilar scattering characteristics. It substantially reduced the data scatter caused by density variations. And it provided a good fit to the theoretically predicted concentration dependence.

REFERENCES:

1. W. M. Doyle, Remote Diffuse Reflectance Analysis for Process Applications, in: *Proceedings of the Conference on Spectroscopy in Process and Quality Control*, East Brunswick NJ, June 7-8, 1999. Also see Axiom Analytical Technical Note AN-920 (in preparation).
2. W. M. Doyle, Signal Level Considerations for Remote Diffuse Reflectance Analysis, Axiom Analytical Technical Note: AN-916 (Rev. A), February 13, 2001.
3. Harald Martens and Tormod Naes, *Multivariate Calibration*, John Wiley & Sons Ltd. Chichester, UK; New York, NY 1989, p. 71.
4. Harald Martens and Tormod Naes, *Ob. Cit.* p. 337.